

Electromagnetic Interactions within Small Particles

The Discrete Dipole Approximation

Tristan Sharp

Small particles can interact with light in non-intuitive ways, scattering much less light than expected at specific angles, or allowing light to resonate within the particle's structure. Predicting these interactions is important to the understanding of global warming, the effects of intergalactic dust particles, and the technology for roadside emissions monitoring. To predict light's interaction with a particle, one would ideally solve Maxwell's equations with boundary conditions specified at the surface of the particle. However, the geometry of many types of small particles is too complex for an analytical treatment.

Soot particles, aggregates of many small carbon spheres, are particularly ugly yet important to understand. Many numerical models have been developed to try to understand light's interaction with soot particles, and not all produce results that agree [2]. One model, the discrete-dipole approximation (DDA) [1], takes an innovative approach. DDA discretizes space by replacing the volume of the particle with a lattice of points, and each point is assigned a polarizability, α . The electric field of the incident light, \mathbf{E}_{inc} , creates an electric dipole at each point, with strength \mathbf{p} proportional to its value of α .

$$\mathbf{p} = \alpha \mathbf{E} \quad (1)$$

If the lattice points coincide with the atoms within the particle, the DDA qualitatively takes on extra physical significance. In an external electric field, an atomic nucleus is displaced slightly from the center of the electron cloud, producing a dipole. In the classical picture, a soot particle truly is a lattice of polarizable atoms. Furthermore, the atomic polarizabilities of various elements have been experimentally measured and tabulated [3, p161].

Once a dipole is produced, the dipole creates its own electric field. For an ideal (non-physical) dipole at the origin, the electric field at \mathbf{r} is given by [3, p155]

$$\mathbf{E}_{dip}(\mathbf{r}) = \frac{1}{4\pi\epsilon_0} \frac{1}{r^3} [3(\mathbf{p} \cdot \hat{\mathbf{r}})\hat{\mathbf{r}} - \mathbf{p}] \quad (2)$$

where $\hat{\mathbf{r}}$ is the unit vector in the direction of \mathbf{r} . This electric field is plotted in Figure 1.

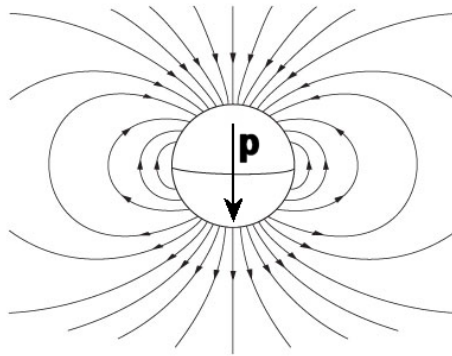


Figure 1: The electric field lines produced by an ideal dipole¹

The electric field produced by each dipole now contributes to the polarizations of its neighbors. Considering all N dipoles in the lattice, the polarization \mathbf{p}_i of the i th lattice point (at \mathbf{r}_i) is proportional to the sum of all the electric field contributions.

$$\mathbf{p}_i = \alpha \left(\mathbf{E}_{inc} + \sum_{k=1, k \neq i}^N \mathbf{E}_{dip,k}(\mathbf{r}_i - \mathbf{r}_k) \right)$$

where $\mathbf{E}_{dip,k}$ is the electric field produced by the k th dipole (located at \mathbf{r}_k). Substituting from (2) and rearranging into a system of linear equations gives

$$\mathbf{A}\mathbf{p} = \mathbf{E}_{inc} \quad (3)$$

The j th, k th element of the N -by- N matrix \mathbf{A} can be defined by

$$\mathbf{A}_{jk}\mathbf{p}_k = \frac{e^{ikr_{jk}}}{r_{jk}^3} \left[k^2 \mathbf{r}_{jk} \times (\mathbf{r}_{jk} \times \mathbf{p}_k) + \frac{1 - ikr_{jk}}{r_{jk}^2} \left[r_{jk}^2 \mathbf{p}_k - 3\mathbf{r}_{jk}(\mathbf{r}_{jk} \cdot \mathbf{p}_k) \right] \right] \quad (j \neq k)$$

$$\mathbf{A}_{jk} = \frac{1}{\alpha} \mathbf{I} \quad (j = k)$$

where \mathbf{I} is the identity matrix, \mathbf{r}_{jk} is the vector from the j th dipole to the k th dipole, or $(\mathbf{r}_j - \mathbf{r}_k)$, and r_{jk} is the magnitude of \mathbf{r}_{jk} . Each element of \mathbf{A} is therefore a 3-by-3 matrix. Notice that the field from the incident light \mathbf{E}_{inc} can be a function of space; for a plane wave of light with wavenumber k , frequency $\omega/2\pi$, and magnitude \mathbf{E}_0 ,

$$\mathbf{E}_{inc} = \mathbf{E}_0 e^{i(\mathbf{k} \cdot \mathbf{r} - \omega t)}$$

Finding the polarizations of each dipole, and the corresponding fields they produce, then becomes a matter of solving the system of equations (3).

Matlab was the tool I chose to implement this model and solve the system of equations. Most important in the decision was the convenience of debugging in Matlab's environment, which I found useful when trying to interpret the model from my references. Moreover, Matlab's convenient system of equations solver, familiar visualizations, and portable 3D figures made the software package desirable.

To construct a lattice of points representative of a soot particle, the program discretizes the space around each carbon sphere. The best positioning for the lattice points to model a sphere is still an open question [1]. There may be an advantage in placing more dipoles around the surface of the sphere, where non-uniformities in polarizations are greatest. However, new computational methods for solving the problem require that the dipoles lie on a regular rectangular lattice. This program opts for a cubic lattice. Dipoles that lie within the sphere are assigned a polarizability of 0.1, and dipoles outside the sphere are assigned (approximately) 0 polarizability.

I first validated the program using simple cases, first with a single dipole in an incident field, then with several interacting dipoles. I next calculated the dipole configuration of a sphere (diameter 1) within a cubic grid, 7 dipoles on a side. In this case, a plane wave of light ($k = 0.2$) is incident from the negative x -direction with polarization in the vertical direction and instantaneous electric field at the origin in the positive z -direction. The result is displayed in Figure 2.

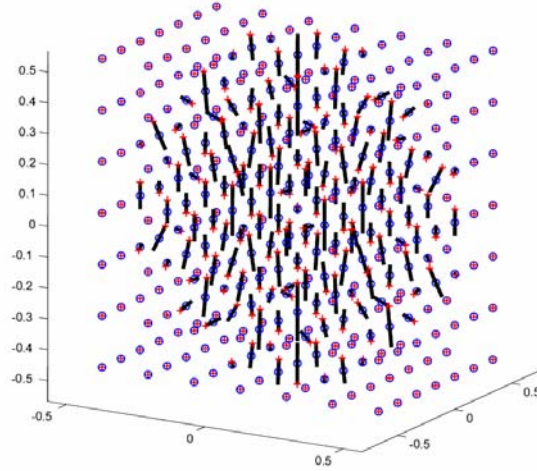


Figure 2: The dipole moments within a 3D sphere, induced by light of wavelength much longer than the diameter of the sphere. The blue circles are the locations of the lattice points. The length of the black lines represent the magnitude of the dipole moments with the red cross signifying the positive direction.

Next, I was able to reproduce the behaviors described in reference 4. Taking a cross section from the y-z plane of the sphere of Figure 2, I obtain the result shown in Figure 3. To reproduce the behavior, I chose α to be .0001 - the curving behavior of the dipoles becomes more pronounced as α increases. For example, when $\alpha = .01$, each sequential dipole essentially cancels the nearby incident field on its own and influences neighboring dipoles to flip entirely. This is shown in Figure 4. As a result, places of zero electric field (as evidenced by the zero dipole moments) result on the inside of the sphere.

Finally, I calculated the dipole configuration for particles made of multiple spheres. (Figure 5) I found that, in general, dipoles with more neighbors were less likely to become polarized away from the vertical. Therefore, the spheres farthest out on the boundaries of the soot particle showed the most erratic polarization behaviors. The largest calculations involved eight spheres, each represented by 216 dipoles.

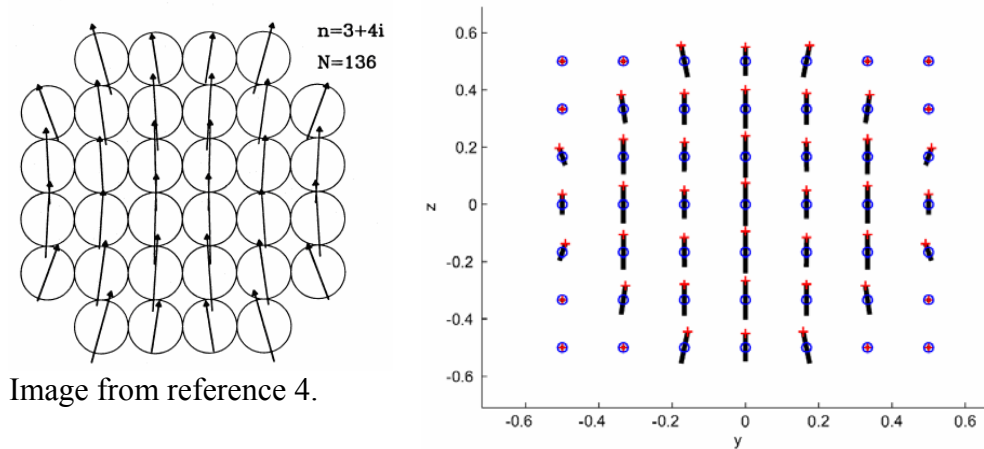


Image from reference 4.

Figure 3: The result at right (polarizability about .0001) reproduces the behavior reported by Draine. The dipoles closest to the surface are deviated inward a small amount. This results from the aggregate electric field produced by the large number of interior dipoles.

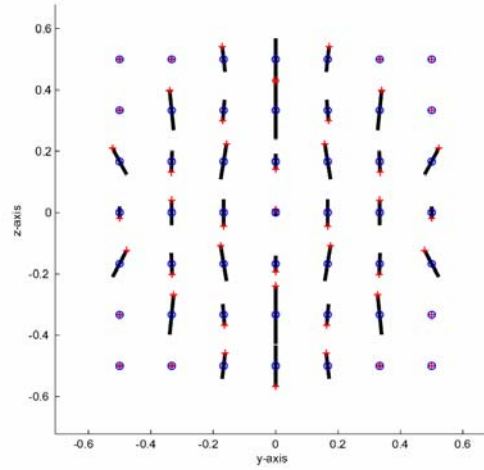


Figure 4: The behavior seen in Figure 3 becomes more pronounced as α grows - until some dipole moments are entirely rotated. The field is zero at the center of the sphere.

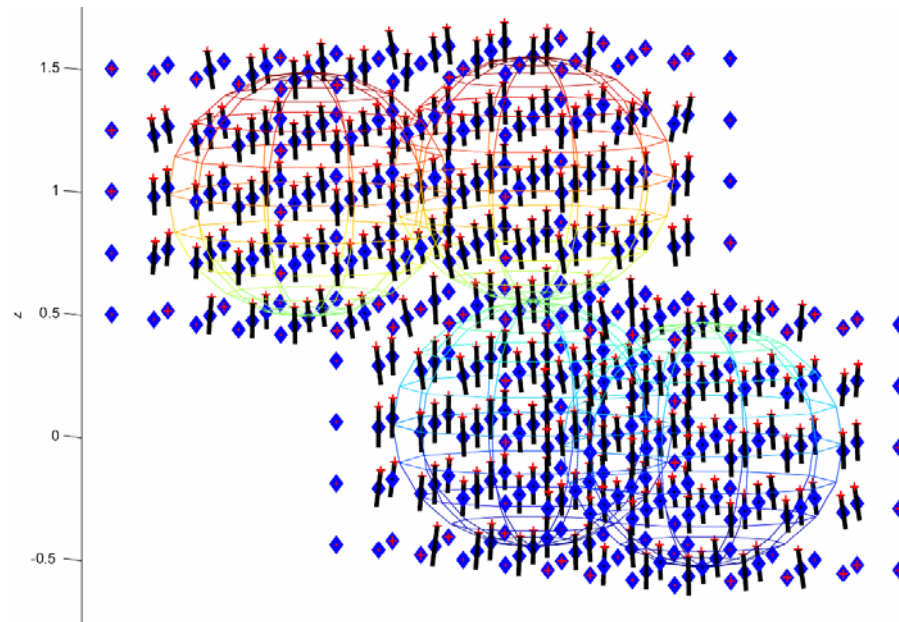


Figure 5: The polarization vectors of dipoles in a soot particle of four touching carbon spheres. Each sphere is represented by a cube, five dipoles on a side. As compared to the seven-by-seven case, there are less dipoles to represent each sphere, and α must be raised to produce a noticeable amount of curving.

To go further, after having solved for the dipole configuration in a given soot particle, I calculated the scattered electric field. Far away from the particle, the scattered field is given by [1]

$$\mathbf{E}_{sca} = \frac{k^2 e^{ikr}}{r} \sum_{j=1}^N e^{-ik\hat{r} \cdot \mathbf{r}_j} (\hat{r}\hat{r} - I) \mathbf{P}_j$$

where \hat{r} is the direction of the detector and I is again the identity matrix. The field scattered from a small soot particle is shown in Figure 5. The scattered field is shown to have a minimum in the direction of incident light polarization. This is an expected result from scattering theory for small particles [6].

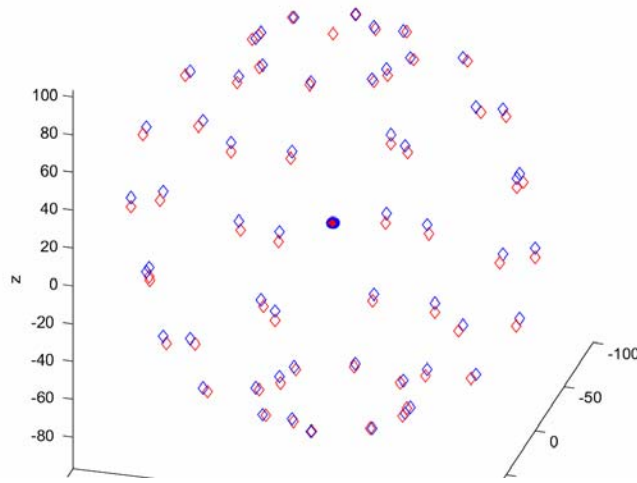


Figure 5: The soot particle (4 particles, each with diameter 1) is shown at the center of 64 detectors (red diamonds) along the surface of a sphere of radius 100. The direction and strength of the electric field is visualized by the direction and distance from red to blue diamond. The electric field is cylindrically symmetric, is everywhere approximately tangent to the sphere, and has minima at the poles.

The program can be extended to model the polarizations in even more complex situations. Changing α for points near the surface of the spheres approximates the situation where the soot is coated with another compound. Also, shrinking the wavelength of light to the scale of the particle will add new behaviors and could investigate resonances within the soot particle. If the magnetic polarizability is assumed to be small, which is normally a valid assumption [3], the information about the electric field could be used to find intensity of light scattered as a function of angle.

Unfortunately, the technique is not as easily extended to larger, more realistic soot particles. In the current implementation, approximating a particle as just eight touching spheres, each represented by a $7 \times 7 \times 7$ lattice, requires creating a full matrix with 52 million values. The matrix scales with the square of the number of lattice points. More recent work [2] in computing techniques for this problem suggest that using a Fourier spectral method could greatly decrease computation time of solving the system of equations (3).

Because of computational limitations, moderate-sized soot particles are often studied in place of large soot particles. To produce results applicable to laboratory measurements of scattering from soot aerosols, a statistically significant number of soot particles must be created and studied. Reference five discusses a method to produce realistic soot particle geometries. In the laboratory, the soot particles tumble randomly in relation to the incident field. Solving for the polarization states for each orientation of each particle can be computationally expensive. Making use of LU decomposition of the matrix \mathbf{A} can facilitate solving (3) multiple times for different \mathbf{E}_{inc} [].

Modeling scattering from small particles is still an open field of research. Relatively straightforward further investigations have the potential to find new physical insights and be applicable to current laboratory research.

References:

- 1 Draine, B T, and Flatau, Piotr J. Discrete-Dipole Approximation for Scattering Calculations. Vol. 11, No 4/April 1994/J. Opt. Soc. Am. A 1491.
- 2 Pascal Van-Hulle, Weill Marc-Emmanuel, Martine Talbaut, Alexis Coppalle. Comparison of Numerical Studies Characterizing Optical Properties of Soot Aggregates for Improved EXSCA Measurements. November 2001.
- 3 Griffiths, David J. *Introduction to Electrodynamics*. Third Edition. Prentice Hall, 1999.
- 4 Draine, B T. The Discrete Dipole Approximation and its Application to Interstellar Graphite Grains. *The Astrophysical Journal*, 333: 848-872, 1988.
(the most concise description of the model, found after implementation)
- 5 Omit O. Koylii,” Yangchuan Xing, and Daniel E. Rosner. Fractal Morphology Analysis of Combustion-Generated Aggregates Using Angular Light Scattering and Electron Microscope Images. *Langmuir* 1996,11, 4848-4854
(possible soot building methods)
- 6 Bohren and Huffman. *Absorption and Scattering of Light by Small Particles*. John Wiley and Sons, Inc. 1983.

¹ The image of a dipole field was modified from a Wikipedia image:
<http://en.wikipedia.org/wiki/Dipole>

For more information:

Goodman and Draine. Application of fast-Fourier-transform techniques to the discrete-dipole approximation. 1991